Heterogeneous & Homogeneous & Bio- & Nano-

CHEMCATCHEM

CATALYSIS

Accepted Article

Title: Rapid and Quantitative Profiling of Substrate Specificity of ω-Transaminases for Ketones

Authors: Sang-Woo Han and Jong-Shik Shin

To be cited as: *ChemCatChem* 10.1002/cctc.201900399

Link to VoR: http://dx.doi.org/10.1002/cctc.201900399

A Journal of

ChemPubSoc Europe

WILEY-VCH

www.chemcatchem.org

10.1002/cctc.201900399

WILEY-VCH

FULL PAPER

Rapid and Quantitative Profiling of Substrate Specificity of ω-Transaminases for Ketones

Sang-Woo Han[a] and Jong-Shik Shin*[a]

ω-Transaminases (ω-TAs) have gained growing attention owing to their capability for asymmetric synthesis of chiral amines from ketones. Reliable high-throughput activity assay of ω-TAs is essential in carrying out extensive substrate profiling and establishing a robust screening platform. Here we report spectrophotometric and colorimetric methods enabling rapid quantitation of ω-TA activities toward ketones in a 96-well microplate format. The assay methods employ benzylamine, a reactive amino donor for ω-TAs, as a cosubstrate and exploit aldehyde dehydrogenase (ALDH) as a reporter enzyme, leading to formation of benzaldehyde detectable by ALDH owing to concomitant NADH generation. Spectrophotometric substrate profiling of two wild-type ω-TAs of opposite stereoselectivity was carried out at 340 nm with 22 ketones, revealing subtle differences in substrate specificities that were consistent with docking simulation results obtained with cognate amines. Colorimetric readout for naked eye detection of the ω-TA activity was also demonstrated by supplementing the assay mixture with color-developing reagents whose color reaction could be quantified at 580 nm. The colorimetric assay was applied to substrate profiling of an engineered ω-TA for 24 ketones, leading to rapid identification of reactive ketones The ALDH-based assay is expected to be promising for high-throughput screening of enzyme collections and mutant libraries to fish out the best ω-TA candidate as well as to tailor enzyme properties for efficient amination of a target ketone.

Introduction

Chiral amines are important building blocks for a wide range of pharmaceutical drugs,[1] spurring development of chemocatalytic [2] and biocatalytic[3] strategies aiming at cost-effective and eco-friendly production of chiral amines with optical purities higher than a pharmaceutical requirement (i.e., > 99.5 % *ee*).[4] In this context, growing research interests for ω-transaminase (ω-TA) witnessed in the last decade are ascribed to its unique catalytic performance affording stereoselective transfer of an amino group from cheap donors, such as isopropylamine and alanine, to prochiral ketones.[5] Thermodynamic limitation in the ω-TA-catalyzed amination of ketones has been identified as a crucial obstacle to implementable process design, which attracted a great deal of research efforts to invent physicochemical and enzymatic methods for driving an equilibrium shift by removing a coproduct.[1b, 3, 5a, 6]

Despite a number of successful examples focused on overcoming the unfavorable reaction thermodynamics,[7] a paucity of naturally occurring ω-TAs available for efficient amination of a target ketone has remained a challenge for scalable process development because of a high enzyme cost.[8] As well exemplified with the sitagliptin production[6b] and reported later elsewhere,[8b, 9] protein engineering of ω-TAs to broaden substrate specificity and improve turnover rate for ketones has been one of the important research goals for enriching product pipelines obtainable by the ω-TA processes.

The success rate of high-throughput screening (HTS) of mutant libraries, constructed by either random mutation or rational design, is highly dependent on fidelity of the assay method in discriminating beneficial activity improvements against neutral and detrimental changes. A number of assay methods have been developed to assess ω-TA activities for amino donors[7b, 10] and acceptors.[11] Depending on the mode of detection, these methods can be classified into three types: 1) direct measurement of differences in physicochemical properties between substrates and products, including conductivity,[10a] UV absorbance[11a] and fluorescence[11g] 2) enzymatic modulation of a coproduct into a measurable readout using oxidase[10b-d] or dehydrogenase[7b, 11b, 11c] and 3) spontaneous chemical conversion of a coproduct into a chromogenic form.[11d-f, 12]

Among the assay methods, the UV absorbance and oxidase-based methods have been successfully applied to mutant library screening to engineer ω-TA activites for bulky ketones by assessing altered activites of mutants for cognate amines.[9b, 9e, 9f] Besides, two methods affording activity assays directly for target ketones have been applied to HTS of metagenomic collection.[12a] These two methods, based on assessment of activities for ketones, employ an amino donor unconventional for ω-TAs, i.e. *o*-xylylenediamine[11d] and 2-(4-nitrophenyl)ethan-1-amine,[11e] whose deamination products undergo spontaneous polymerization or imine formation, respectively, leading to a colored precipitate. A potential drawback of these methods is that the amines used in the assays are not generally accepted amino donors for ω-TAs and thereby a resulting enzyme candidate displaying a strong colorimetric readout could be a false positive showing an activity improvement for the amino donor rather than the target ketone.

Here we aimed at developing a generally applicable assay method for quantitative activity measurements of both *S*- and *R*-selective ω-TAs toward ketones using a universal amino donor whose deamination product is detectable spectrophotometrically or colorimetrically after enzymatic modulation. We explored a possibility that the new assay method can be exploited for rapid characterization of substrate specificity of a given ω-TA for ketones and eventually for application to HTS of mutant libraries.

[a] Dr. S.-W. Han, Prof. Dr. J.-S. Shin
Department of Biotechnology
Yonsei University
Yonsei-Ro 50, Seodaemun-Gu, Seoul 03722 (South Korea)
Fax: (+82) 2-362-7265
E-mail: enzymo@yonsei.ac.kr

Supporting information for this article is given via a link at the end of the document.((Please delete this text if not appropriate))

10.1002/cctc.201900399

Results and Discussion

Feasibility test of the enzyme assay

To develop an activity assay method for both *S*- and *R*-selective ω-TAs toward ketones, the amino donor substrate used in the assay reactions should be achiral and signal amplification of the deamination product should be possible without interference by the ketone substrate. We posited that benzylamine (**3**) would fulfil the requirements to be considered as an ideal amino donor for the enzyme assay we intended to develop. First, **3** is a reactive amino donor for ω-TAs known to date.[13] Based on literature surveys, activity data for **3** are available with sixteen ω-TAs, i.e. 12 *S*-selective and 4 *R*-selective ones, and they display 10 to 260 % activities for **3** relative to α-methylbenzylamine (α-MBA), a typical amino donor for ω-TAs (Table S1). The only exception is the *R*-selective ω-TA from *Arthrobacter* sp., i.e. 3 % relative activity, although its engineered variant shows 28 % activity.[14] Second, the deamination product of **3**, i.e. benzaldehyde (**4**), is chemically different from ketone and thereby can be specifically quantified by an aldehyde dehydrogenase (ALDH) as a reporter in colorimetric as well as spectrophotometric manners (Scheme 1). ALDH oxidizes **4**, generated from the ω-TA reaction, into benzoic acid (**5**) at the expense of reduction of NAD^+, leading to formation of NADH detectable spectrophotometrically as an increase in UV absorbance at 340 nm with a molar extinction coefficient, $\varepsilon = 6220\ M^{-1}\,cm^{-1}$ (method 1). Colorimetric visualization of the ω-TA activity can be also achieved by supplementing the assay mixture with nitroblue tetrazolium (NBT) and phenazine methosulfate (PMS) that lead to formation of blue-purple NBT-formazan, detectable at 580 nm (ε=12300 $M^{-1}cm^{-1}$)[15] as shown in method 2.

Feasibility of the proposed assay method is contingent upon the reaction conditions where ALDH is active only for **4** and totally inactive for ketones used as substrates for ω-TA as listed in Scheme 2. We used ALDH cloned from *Azospirillum brasilense* (GenBank™ accession number: AB241137)[16] and found that the ALDH efficiently catalysed oxidation of **4** in the presence of NAD^+ with a specific activity of 4.8 ± 0.3 U mL^{-1} μM-enzyme^{-1} (Fig. S1). In contrast, the ALDH showed a non-detectable activity for acetophenone (**1n**), a typical ketone substrate for ω-TAs (Fig. S1). In addition to **1n**, ALDH showed negligible oxidative activities for all the 24 ketones shown in Scheme 2 (i.e., < 0.2 % activity relative to that for **4**).

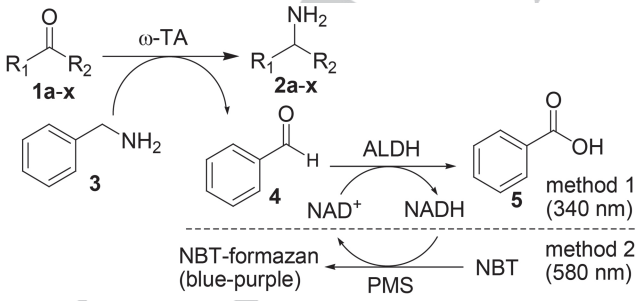

Scheme 1. ALDH-based assay of ω-TA activity for ketone through spectrophotometric (method 1) or colorimetric (method 2) detection of **4**.

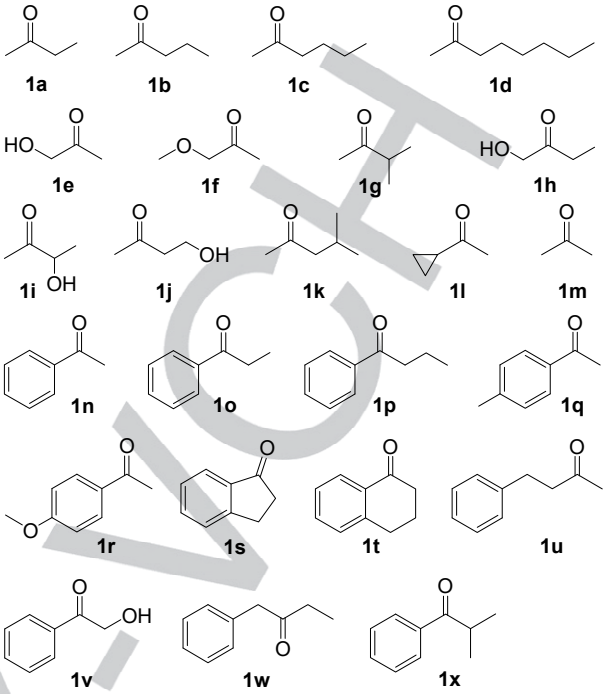

Scheme 2. Alkyl (**1a**-**m**) and arylalkyl (**1n**-**x**) ketones used in this study.

The fidelity of the coupled enzyme assay for precise quantitative measurement of ω-TA activity in terms of readout from the ALDH reaction requires that the reporter enzyme reaction should be irreversible and thereby **4** is completely converted to **5**. Otherwise, the coupled enzyme assay would lead to underestimation of the ω-TA activity. Thermodynamic equilibrium of the ALDH reaction between acetaldehyde and acetic acid is known to be strongly shifted to acetic acid.[17] Likewise, ALDH was found to be unable to catalyse reduction of **5** in the presence of NADH (Fig. S2), indicating that conversion of **5** to **4** by a reducing power of NADH is thermodynamically unfavorable. It is notable that ALDH was also incapable of catalysing reduction of 22 ketones tested (**1a**-**1v**, data not shown), indicating ALDH is totally inactive for ketones in both oxidative and reductive reactions. Besides the ALDH cloned from *A. brasilense*, the ALDH from *Escherichia coli* (i.e. AldH)[18] was also observed to be devoid of any activities for ketones in Scheme 2 (data not shown).

Another important requirement for the quantitative real-time monitoring of ω-TA activity is that **4** should be instantly consumed by the reporter enzyme as soon as it is formed, so the generation rate of **4** (V_4) becomes the same as that of NADH (V_{NADH}). To achieve this condition, the reporter enzyme activity should be in excess over the ω-TA activity. To determine such a threshold ALDH level required to overwhelm the ω-TA activity, V_{NADH} was measured at varying concentrations of ALDH under a fixed concentration of ω-TA (Fig. 1). Time-course monitoring of optical density at 340 nm (OD_{340}) was done for 10 min, which showed linear increases in OD_{340} during the assay time ($r^2 > 0.97$; Fig. S3). The V_{NADH} values, obtained by linear regressions of the OD_{340} data sets, showed a hyperbolic dependence on the ALDH

10.1002/cctc.201900399

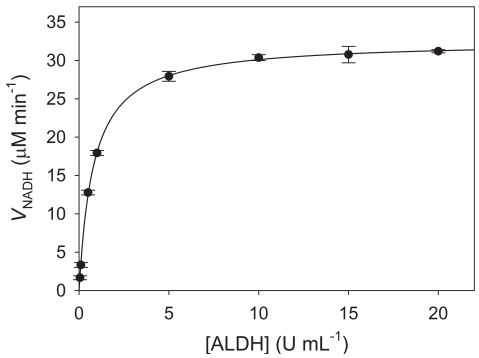

Figure 1. Determination of a threshold concentration of ALDH for accurate measurement of ω-TA activity. Assay conditions: **1n** (10 mM), **3** (100 mM), NAD^+ (2 mM), ω-TA ($OATA_{W58L}$, 1 μM) and ALDH (0.05 - 20 U mL^{-1}).

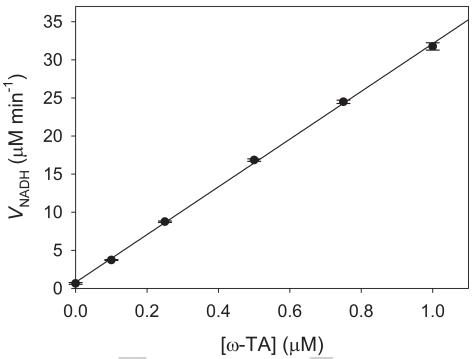

Figure 2. Spectrophotometric measurement of the ω-TA activity in the assay mixtures containing different doses of $OATA_{W58L}$. Assay conditions: **1n** (10 mM), **3** (100 mM), NAD^+ (2 mM), $OATA_{W58L}$ (0-1 μM) and ALDH (10 U mL^{-1}).

concentration, yielding 32.5 μM min^{-1} as an upper limit which can be regarded as an actual V_4. Since V_{NADH} levelled off above 5 U mL^{-1} of ALDH, we set 10 U mL^{-1} as a working concentration for the ALDH excess condition in further enzyme assays unless V_4 exceeded 32.5 μM min^{-1}. Note that the ω-TA used in the enzyme assay was an engineered *S*-selective enzyme from *Ochrobactrum anthropi* carrying a W58L substitution ($OATA_{W58L}$) which was rationally introduced to impart activity improvements for ketones in the previous study.[9c]

Verification of the ALDH-based assay

To verify the ALDH excess condition for precise measurement of ω-TA activity, we examined how V_{NADH} responded to varying concentrations of $OATA_{W58L}$ at 10 U mL^{-1} ALDH. As observed in Fig. S3, linear increases in OD_{340} were also observed during the 10-min assay time irrespective of the ω-TA concentrations (r^2 > 0.99; Fig. S4). We expected a linear correlation between the concentration of ω-TA and V_{NADH} when the assay conditions fulfilled $V_4 \approx V_{NADH}$. Indeed, the V_{NADH} values showed a strong linear dependence on the ω-TA concentration (r^2 = 0.99), illustrating reliability of the assay method for quantitative measurement of ω-TA activity (Fig. 2). Limit of detection (LOD) for the concentration of $OATA_{W58L}$, calculated from the regression results, was 20 pM which corresponds to a reaction rate of 0.6 μM min^{-1}. Therefore, this method provides reliable measurement of ω-TA activity as long as V_{NADH} is higher than 0.6 μM min^{-1} under the ALDH excess condition.

In the conventional HPLC analysis to measure ω-TA activity for ketones (e.g., amination of **1n** using alanine or isopropylamine as an amino donor), UV detection of the produced amine (e.g., α-MBA (**2n**)) usually permits reliable quantitation of the product formation higher than 10 μM.[9c, 19] In this case, an experimental LOD in terms of a reaction rate is over 10 μM min^{-1} when the reaction is allowed for a minute which is usually regarded as a minimal time required to keep enzyme reactions running reliably. Therefore, the ALDH-based assay is at least more than 15-fold sensitive than the HPLC method. In addition to the higher detection sensitivity, benefit of the ALDH-based method becomes more striking when a target substrate is non-chromogenic alkyl ketones (e. g. **1a-m**) because UV detection of the resulting amines requires laborious derivatization with a chromogenic reagent such as a Marfey's reagent.[9c, 19]

To corroborate the reliability of the proposed assay, we compared the assay results between HPLC and ALDH-based methods. To this end, we employed two wild-type ω-TAs, i.e. *S*-selective one from *Paracoccus denitrificans* (PDTA)[13d] and *R*-selective one from *Arthrobacter* sp. (ARTA).[20] For both enzymes, real-time spectrophotometric measurement of NADH generation led to reaction rates close to those obtained by end-point HPLC analysis of the produced amine (Fig. 3). It is notable that the ALDH-based method can be applied to both enantiocomplementary ω-TAs under the same reaction conditions because the amino donor, **3**, is achiral.

In addition to the spectrophotometric measurement, colorimetric detection of the ω-TA activity could be also carried out when the assay mixture was supplemented with NBT and PMS. In contrast to the linear increase of OD_{340} within the entire assay time as shown in Fig. S4, onset of such a linear increase in optical density at 580 nm (OD_{580}) became retarded up to 1.5 min

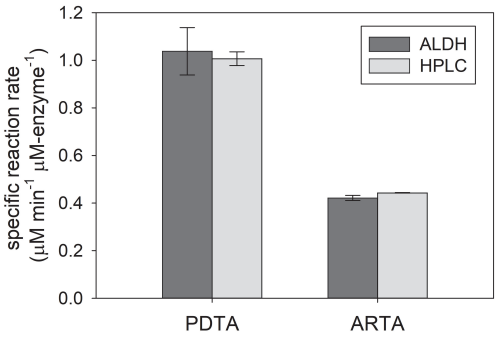

Figure 3. Comparison of the ALDH-based assay with the HPLC method. Specific reaction rate represents an initial reaction rate normalized by a ω-TA concentration. Reaction conditions: **1n** (5 mM), **3** (50 mM), NAD^+ (2 mM), ω-TA (5 and 15 μM for PDTA and ARTA, respectively) and ALDH (10 U mL^{-1}). For the HPLC method, produced amines after a 10-min reaction were analyzed by chiral HPLC.

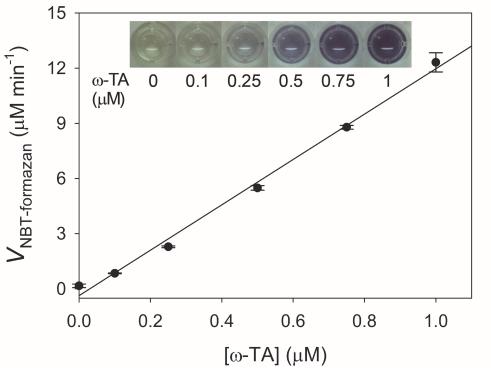

Figure 4. Colorimetric measurements of the ω-TA activity. Assay conditions were the same as those for Figure 2 except that the assay mixtures were supplemented with NBT (122 μM) and PMS (16 μM). The inset figure shows visual images of each microplate well after 10-min reaction.

(Fig. S5). This is presumably because the color-developing reaction (i.e., reduction of NBT to NBT-formazan by PMS and NADH) is slower than the ALDH reaction and/or follows complex kinetics consisting of multiple reaction steps.[21] We did not optimize the assay conditions to speed up the color reaction. Instead, linear regression to obtain the formation rate of NBT-formazan ($V_{NBT\text{-}formazan}$) was carried out at a 1.5-10 min time range where a time-dependent linear increase in OD_{580} was observed (r^2 > 0.99; Fig. S5). The $V_{NBT\text{-}formazan}$ values were plotted against ω-TA concentrations (Fig. 4), resulting in a strong linear relationship (r^2 = 0.99). In line with the delay in onset of the linear increase in OD_{580}, the assay conditions of $V_{\mathbf{4}} \approx V_{NADH} > V_{NBT\text{-}formazan}$ led the slope in Fig. 4 to become 2.54-fold lower than that in Fig. 2. This result indicates that the $V_{NBT\text{-}formazan}$ value obtained from the colorimetric assay should be multiplied by a scaling factor of 2.54 to evaluate an actual $V_{\mathbf{4}}$. Visual inspection of the color intensity in each well is qualitatively consistent with the OD_{580} measurements.

Spectrophotometric substrate profiling of ω-TA

Based on the reliability of the ALDH-based assay, we carried out substrate profiling of PDTA and ARTA for 22 ketones (**1a**-**v**) using the spectrophotometric detection of NADH (Table 1). Compared to **1n**, three ketones (i.e., **1e**, **1f** and **1u**) showed higher reactivities with the *S*-selective PDTA. The *R*-selective ARTA showed such higher activities for **1f**, **1k** and **1v** than it did for **1n**. These results indicate different active site structures that define the mode of substrate binding and the efficiency of catalytic turnover, which can be taken for granted considering distinct phylogenetic evolution of the two enzymes. Note that *S*- and *R*-selective ω-TAs belong to a subgroup II of α-family and a D-alanine transaminase family, respectively, based on a classification of PLP-dependent enzymes by Christen and Mehta.[22] Likewise, the two enzymes belong to different subclasses based on another classification system,[23] i.e. fold-type I and IV for *S*- and *R*-selective ω-TAs, respectively.

To gain more insight into how substrate specificities of the two enzymes are different, we scored the relative activity for each ketone (i.e. $V_{rel} = V_{PDTA}/V_{ARTA}$) on a log scale with a base of 2 (Table 1). In the case of 13 alkyl ketones (**1a**-**m**), V_{rel} did not show a general trend but was dependent on a specific substrate structure (i.e., 7 negative and 6 positive $\log_2 V_{rel}$ values). But when the alkylamines were divided into two groups depending on the presence of a non-alkyl substituent flanking the carbonyl group, a rule-of-thumb difference in the substrate specificities could be captured. For ketones carrying both alkyl substituents (i.e., **1a**-**d**, **1g** and **1k**-**m**), ARTA showed a higher activity than PDTA did except the smallest and the largest ketones (i.e., **1m** and **1d**, respectively). In constrast, the two enzymes exhibited an opposite trend (i.e., $\log_2 V_{rel} > 0$) for ketones carrying a non-alkyl substituent (i.e. **1e**-**f** and **1h**-**j**) except **1j**.

Similarly, positive $\log_2 V_{rel}$ values were observed for arylalkyl ketones (i.e., **1n**-**v**) except **1r** and **1v**. Besides the negative $\log_2 V_{rel}$ value, **1v** attracted our attention because of an opposite trend of the two ω-TAs in the activities relative to **1n** (i.e. $V_{\mathbf{1v}}/V_{\mathbf{1n}}$). Note that the $V_{\mathbf{1v}}/V_{\mathbf{1n}}$ values are 0.29 and 2.4 for PDTA and ARTA, respectively. Consistent with the spectrophotometric assay results, HPLC analysis of the produced amines showed that PDTA accepted **1n** as an amino acceptor better than **1v** while ARTA did the other way around (Table 2). Note that the cosubstrate used for these ω-TA reactions was isopropylamine which is a popular amino donor for amination of ketones owing to easy removal of a coproduct by vacuum evaporation for equilibrium shift. Enantiomeric excesses (*ee*) of the produced amines were > 99 % in all the chiral analyses. Due to the inversed

Table 1. Substrate specificities of PDTA and ARTA for ketones examined by the spectrophotometric assay.[a]

Ketone	Specific reaction rate (V) (μM h^{-1} μM-enzyme^{-1})		$\log_2\left(\frac{V_{PDTA}}{V_{ARTA}}\right)$
	PDTA	ARTA	
1a	3.5 ± 0.4	4.7 ± 0.6	-0.3
1b	3.2 ± 0.4	4.9 ± 0.7	-0.5
1c	6.0 ± 0.8	28 ± 1	-2.3
1d	40 ± 10	12 ± 2	1.7
1e	120 ± 20	13 ± 2	3.2
1f	110 ± 20	72 ± 5	0.7
1g	3.7 ± 0.1	5.0 ± 1.3	-0.5
1h	5.2 ± 0.3	3.2 ± 1.3	0.7
1i	8.9 ± 0.2	5.8 ± 1.0	0.6
1j	5.0 ± 0.7	9.2 ± 1.0	-1.0
1k	4.5 ± 0.2	34 ± 1	-3.3
1l	3.5 ± 0.7	4.3 ± 0.5	-0.3
1m	8.8 ± 0.4	3.8 ± 0.5	1.2
1n	63 ± 4	28 ± 0.5	1.1
1o	14 ± 1	2.7 ± 0.5	2.3
1p	11 ± 0.2	2.6 ± 0.6	2.0
1q	16 ± 1	10 ± 2	0.7
1r	8.9 ± 0.8	10 ± 4	-0.2
1s	24 ± 2	4.9 ± 0.6	2.3
1t	18 ± 3	1.3 ± 0.7	3.7
1u	96 ± 3	16 ± 1	2.6
1v	18 ± 1	67 ± 5	-1.7

[a] Assay conditions: ketone (5 mM), **3** (50 mM), DMSO (10 % (v/v)), NAD^+ (2 mM), ω-TA (5 or 15 μM) and ALDH (10 U mL^{-1}).

10.1002/cctc.201900399

Table 2. HPLC measurements of ω-TA activities of PDTA and ARTA for amination of **1n** and **1v** as well as deamination of their cognate amines.

ω-TA	Amination reaction rate[a] (μM h^{-1} μM-enzyme^{-1})		V_{1v}/V_{1n}	Deamination reaction rate[b] (mM h^{-1} μM-enzyme^{-1})		V_{2v}/V_{2n}
	1n	**1v**		**2n**	**2v**	
PDTA	32	9.7	0.30	75	0.52	6.9×10^{-3}
ARTA	4.7	15	3.2	7.8	6.2	0.79

[a] Reaction conditions: ketone (5 mM), isopropylamine (50 mM) and ω-TA (5 μM). After 90-min reaction, produced amines were analyzed by chiral HPLC.
[b] Reaction conditions: (*S*) or (*R*)-amine (10 mM), pyruvate (10 mM) and ω-TA (0.1 or 1 μM for **2n** or **2v**, respectively). After 10-min reaction, produced ketones were analyzed by reverse-phase HPLC.

assigning priority in the Cahn-Ingold-Prelog rule for **2n** and **2v**, amines produced by PDTA were (*S*)-**2n** and (*R*)-**2v** while those by ARTA were (*R*)-**2n** and (*S*)-**2v**. The V_{1v}/V_{1n} values determined by the HPLC analysis are in good agreements with those obtained by the spectrophotometric assay, indicating that the choice of an amino donor, at least either **3** or isopropylamine, does not significantly affect the measurement of relative activities for ketones. This result broadens applicability of the ALDH-based assay to consideration of process scale-up for amine synthesis using isopropylamine.

The opposite preferences of the two ω-TAs for **1n** and **1v** intrigued us to measure enzyme activities for cognate amines of the two ketones (i.e., **2n** and **2v**). The preference of PDTA for **1n** over **1v** was found to be more striking when the activities for their cognate amines were compared (Table 2). PDTA showed only 0.7 % activity for (*R*)-**2v** relative to (*S*)-**2n**, which is a drastic activity reduction for 30 % relative activity of **1v** over **1n**. This is in line with our previous observation with PDTA that the steric constraint in the small substrate binding pocket (i.e., S pocket) becomes stronger for amino donors compared with amino acceptors.[24] In contrast, such an abrupt activity drop did not occur with ARTA and instead activities for (*R*)-**2n** and (*S*)-**2v** were not very different.

These results of the V_{1v}/V_{1n} and V_{2v}/V_{2n} values in Table 2 prompted us to carry out substrate docking simulations, which we expected to provide structural insights into how the two ω-TAs ended up with differential relative activities for the cognate substrates. The whole catalytic cycle of transaminase reactions consists of oxidative deamination of an amino donor and reductive amination of an amino acceptor which are mediated by a pyridoxal 5′-phosphate form of the enzyme (E-PLP) and a pyridoxamine 5′-phosphate form (E-PMP), respectively.[25] Therefore, reliable docking simulations of the donor-acceptor substrate pairs require precise active site structures of both enzyme forms. However, X-ray structures of only the E-PLP form of the two ω-TAs are available yet.[26] This led us to carry out molecular docking of donor substrates only, i.e. **2n** and **2v** (Fig. 5). The docking models of **2n** clearly show that spatial orientations of the reacting amine enantiomer and the PLP moiety in the two enantiocomplementary ω-TAs are mirror images of each other. The distance between the C4′ of PLP and the nitrogen of the amine substrate (C4′-N) was 3.0 and 3.2 Å for (*R*)-**2n** in ARTA and (*S*)-**2n** in PDTA, respectively. In the previous report, the C4′-N distance was 2.9 Å in a docking model of (*S*)-**2n** in OATA.[19] Considering that **2n** is a typical amino donor for ω-TAs, these results suggest that the optimal length of C4′-N in a productive Michaelis complex is around 3 Å. Note that the optimal distance between the electrophilic carbon center and the N of the nucleophile in a transition state for a nucleophilic attack is known to be 2.5 Å.[27] We examined whether the differential V_{2v}/V_{2n} values, depending on the ω-TA, could be explained by how much the C4′-N distance for **2v** deviated from the optimal distance observed with **2n**. The docking pose of (*S*)-**2v** in ARTA indicates that C4′-N is marginally influenced by the additional steric burden in the S pocket imposed by the hydroxyl group of **2v** (Fig. 5A). The C4′-N distance in the Michaelis complex with (*S*)-**2v** is only 0.2 Å longer than that with (*R*)-**2n** and the bound (*S*)-**2v** is found to be stabilized by a H-bond between the hydroxyl hydrogen of (*S*)-**2v** and the nitrogen in the peptide bond between T283 and A234. In contrast, the S pocket of PDTA is not spacious enough to allow such an accommodation of the

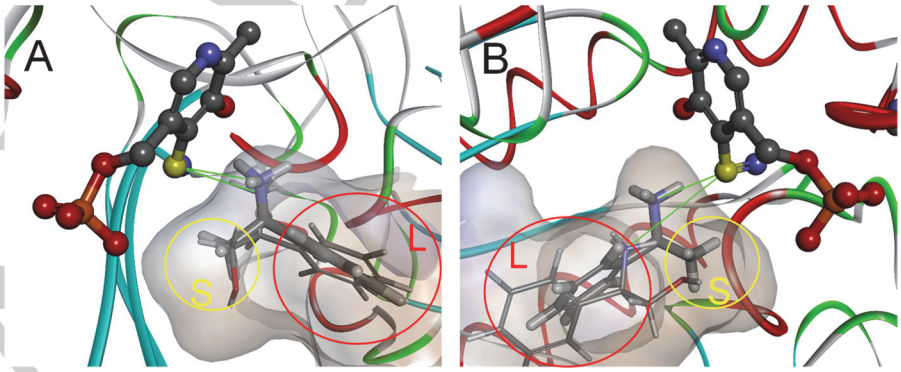

Figure 5. Molecular docking of **2n** and **2v** to the E-PLP forms. (**A**) Docking poses of (*R*)-**2n** and (*S*)-**2v** in ARTA. (**B**) Docking poses of (*S*)-**2n** and (*R*)-**2v** in PDTA. The internal aldimine moiety from PLP to a Schiff base nitrogen is shown in a ball-and-stick model. For visual clarity, hydrogens are omitted in the PLP where the C4′ carbon is colored in yellow. Thick and thin sticks represent **2n** and **2v**, respectively. Active sites are shown as a Connolly surface. Yellow and red circles represent the small (S) and large (L) binding pockets, respectively. Green lines represent a C4′-N distance. Color code for atoms: dark grey, light grey, blue and red for C, H, N and O, respectively.

10.1002/cctc.201900399

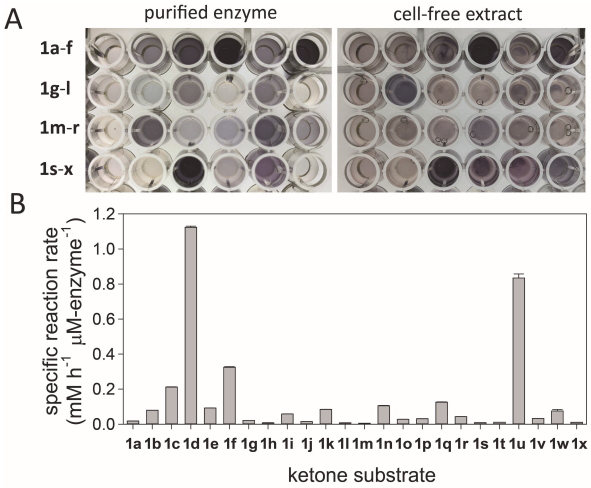

Figure 6. Colorimetric assay for substrate profiling of $OATA_{L57A/W58A}$ with ketones. (**A**) Photo images of the 96-well plate taken after 20 and 5-min reactions with purified enzyme and cell-free extract, respectively. (**B**) Measurement of the reaction rate of purified enzyme by monitoring increase in OD_{580}. Reaction conditions: **1a-x** (5 mM), **3** (50 mM), NAD^+ (2 mM), DMSO (10 % (v/v)), purified enzyme or cell-free extract (7.5 μM or 0.95 mg-protein mL^{-1}, respectively), ALDH (15 U mL^{-1}), NBT (122 μM) and PMS (16 μM).

hydroxymethyl group of (*R*)-**2v** and the resulting C4′-N is 1.2 Å longer compared with that for (*S*)-**2n** (Fig. 5B). The docking models are in good accordance with the relative enzyme activities of both ω-TAs and illustrate well how the subtle difference in the S pocket geometry leads to such a dramatic change in the substrate preference.

Colorimetric substrate profiling of ω-TA

In addition to the spectrophotometric method, the ALDH-based assay also provides colorimetric detection of ω-TA activities for ketones (method 2 in Scheme 1). We applied the colorimetric method to rapid visualization of substrate preference of an OATA mutant carrying L57A and W58A substitutions ($OATA_{L57A/W58A}$) which was engineered to accept bulky ketones such as **1o** and **1p** in a previous study.[8b] Substrate specificity of $OATA_{L57A/W58A}$ has not yet been characterized using a wide range of ketones besides **1n-p**. We run the colorimetric assay of purified $OATA_{L57A/W58A}$ with all the 24 ketones shown in Scheme 2 and the image of the 96-well plate was taken after 20-min reaction (Fig. 6A, left image). Visual inspection of the color intensity led to rapid evaluation of substrate specificity for ketones in a qualitative manner; 1) strong ω-TA activities for **1c**, **1d**, **1f** and **1u**, 2) low activities for **1a**, **1g**, **1h**, **1j**, **1l**, **1m**, **1s**, **1t** and **1x** and 3) moderate activities for the rest 11 ketones. For rapid characterization of a number of enzymes, cell-free extract is a favored formulation over purified enzyme. The colorimetric assay using cell-free extract led to considerable background development (Fig. 6A, right image). However, the background was low enough to pinpoint highly reactive ketones such as **1d** and **1u**.

The colorimetric method enables quantitative activity measurements in terms of a reaction rate through time-course monitoring of the color development at 580 nm. To this end, OD_{580} data obtained with purified enzyme were subjected to linear curve fitting for the reaction rate evaluation (Fig. 6B). Consistent with the visual inspection, **1d** and **1u** were ranked top 2 reactive ketones. Reactivity improvements for **1d** and **1u** by the L57A/W58A substitutions were remarkable and the fold-increases in the activities of the engineered variant for the two ketones, compared with those of the wild-type OATA,[8b] were 1020 and 270, respectively. It is notable that the activities of $OATA_{L57A/W58A}$ for **1d** and **1u** were 280 and 90-fold, respectively, higher than those of PDTA displaying the same *S*-stereoselectivity.

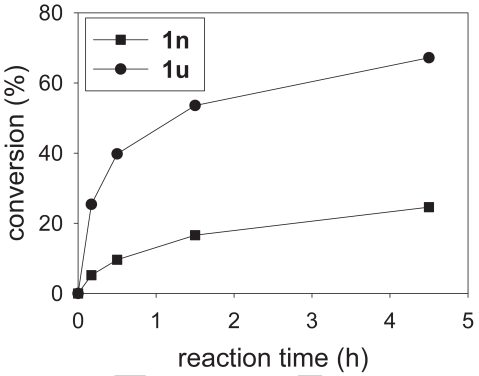

Figure 7. Time-course monitoring of amination of **1n** and **1u**. Reaction conditions: ketone (5 mM), isopropylamine (100 mM) and $OATA_{L57A/W58A}$ (40 μM).

Taken together, the substrate profiling results indicate that $OATA_{L57A/W58A}$ is promising for efficient amination of **1d** and **1u**. To examine whether the colorimetric assays provide reliable enzyme-ketone matching information available for practical amine synthesis, we carried out amination of **1u**, in comparison with **1n**, using isopropylamine (20 molar eq. to the ketone substrate) as an amino donor (Fig. 7). Conversion of **1u** to (*S*)-**2u** reached 67 % at 4.5 h even without coproduct removal. In contrast, conversion of **1n** to (*S*)-**2n** was only 25 % at the same reaction time.

Conclusions

Rapid and precise identification of an optimal ω-TA, displaying desirable kinetics and stability for a target ketone, out of commercially available enzyme collections or lab-made mutant libraries is a crucial step for successful process development of asymmetric synthesis of chiral amines using ω-TAs. The ALDH-based assay is generally applicable to ketones regardless of chemical structures. Moreover, the assay method can be expanded to activity measurement for keto acids as well as a limited range of aldehydes for which the ALDH used in the activity assay is not active. For example, benzaldehyde dehydrogenase from *Pseudomonas putida* ATCC 12633 is known to exhibit narrowly defined substrate specificity for aldehydes.[28] The proposed method offers flexbility in selecting a detection mode, i.e. spectrophotometric and colorimetric, whose choice is dependent on trade-off between precise activity quantitation and rapid target enzyme identification. It is worth noting that the colorimetric assay affords rapid naked-eye inspection of a number of reaction samples, eliminating a need for any expensive analytical equipment to capture an invisible product readout.

Experimental Section

Chemicals

1k and **1p** were purchased from Alfa Aesar (Ward Hill, MA, USA). **4**, **1m** and DMSO were obtained from Duksan Pure Chemicals Co. (Ansan, South Korea). Isopropylamine was obtained from Junsei Chemical Co. (Tokyo, Japan). All other chemicals were purchased from Sigma-Aldrich Co. (St. Louis, MO, USA) and of the highest purity available.

Protein expression and purification

The ω-TAs, i.e. PDTA,[13d] ARTA,[29] $OATA_{W58L}$[9c] and $OATA_{L57A/W58A}$,[8b] were cloned in a pET28(+) expression vector (Novagen) as described in our previous studies. Cultivation of *E. coli* BL21(DE3) cells transformed with the plasmids, overexpression of the His_6-tagged ω-TAs and protein purification were carried out as described elsewhere with minor modifications.[8b] Standard reaction conditions for activity assay were 10 mM (*S*) or (*R*)-**2n** and 10 mM pyruvate in 50 mM Tris buffer (pH 7). The enzyme reaction was stopped after 10 min by adding acetonitrile and then **1n** was analyzed by HPLC. Preparation of purified ALDH was performed as described elsewhere.[18] One unit of ALDH was defined as the enzyme amount required to oxidize 1 μmol of **4** to **5** in 1 min at 10 mM **4**, 2 mM NAD^+ and 50 mM Tris buffer (pH 7). Reaction progress was monitored by a UV spectrophotometer (UV-1650PC, Shimadzu Co.) at 340 nm and the initial rate was obtained by a linear regression of the UV absorbance data within the time interval showing a linear increase. Protein concentrations were determined by measuring UV absorbance at 280 nm. Molar extinction coefficients of the purified proteins were obtained by a protein extinction coefficient calculator (http://www.biomol.net/en/tools/proteinextinction.htm). The ε values of homodimeric ω-TAs and were 101885 M^{-1} cm^{-1} for ARTA, 122576 M^{-1} cm^{-1} for PDTA and 67076 M^{-1} cm^{-1} for both $OATA_{W58L}$ and $OATA_{L57A/W58A}$. The ε value of the homotetrameric ALDH was 174220 M^{-1} cm^{-1}.

Coupled enzyme assay

All the coupled enzyme assays were conducted in 50 mM Tris buffer (pH 7) at 37 °C on a 96-well microplate and a typical reaction volume was 200 μL. Concentrations of NADH or NBT-formazan were determined by measuring OD_{340} or OD_{580}, respectively, using a microplate reader (BioTek Instruments, Inc). Initial rates were obtained from at least three independent measurements by linear regression of the optical density data within the time range showing a linear increase. LOD of the ω-TA concentration was calculated by LOD = $3.3\sigma/S$ where σ and *S* are the standard deviation of y-intercept and the slope of the regression curve.[30]

Molecular modeling

Molecular modeling was carried out using a Discovery Studio package (version 3.5.0, Accelrys) as described before with minor modifications.[8b] Crystal structures of PDTA (PDB ID: 4GRX)[26a] and ARTA (PDB ID: 3WWH)[26b] were used for docking simulations of **2n** and **2v**. Both ω-TAs assume a homodimeric structure. In 4GRX, two active site arginines (R415) form different conformations as previously reported.[9c] One of the two active sites, harboring R415 in an outward conformation (i.e., pointing away from PLP), was chosen for docking simulation. In the case of 3WWH, both active site arginines (R138) assume an inward conformation (i.e., pointing toward PLP). Therefore, the active site was modified by a R138A substitution and then used for docking simulation to allow hydrophobic substituents of the arylalkylamines to be accommodated in the L pocket. In both crystal structures, the C4′-N linkage in the internal aldimine is assigned to a single bond instead of a double bond. To make the C4′-N bond close to an actual Schiff base linkage, hybridization states of the C4′ and N atoms in the internal aldimine were changed to sp^2. Docking simulations were carried out using CDOCKER module under a default setting (2000 steps at 700 K for a heating step; 5000 steps at 300 K for a cooling step; 8 Å grid extension) within the active site defined by the Binding-Site module.

Asymmetric synthesis of chiral amines

Reactions were carried out in a 1.8-mL glass vial under magnetic stirring at 37 °C. Total reaction volume was 1.5 mL. Reaction conditions were **1n** or **1u** (5 mM), isopropylamine (100 mM), DMSO (10 % (v/v)) and $OATA_{L57A/W58A}$ (40 μM) in 50 mM Tris buffer (pH 7). Aliquot of the reaction mixture (typically 100 μL) was taken at predetermined reaction times and mixed with 37.5 μL of 16 % (v/v) perchloric acid to stop the reaction. Enzyme precipitate was removed by centrifugation (13000 rpm, 10 min) and then the supernatant was subjected to HPLC analysis. Conversion was measured by chiral analysis of the produced (*S*)-amine.

HPLC analysis

All the HPLC analyses were carried out using an Alliance HPLC system (Waters Co.) or a 1260 Infinity HPLC system (Agilent Technologies). Quantitative analyses of **1n** and **1v** were performed using a Symmetry C18 column (Waters Co.). **2v** was analyzed on the same column after derivatization with 1-fluoro-2,4-dinitrophenyl-5-L-alanine amide (Marfey's reagent) as described elsewhere.[8b] Chiral analyses of **2n** and **2u** were carried out using Crownpak CR(-) and Crownpak CR-I(+) columns (Daicel Co.), respectively. Details of the HPLC analyses are described in the Supporting Information.

Acknowledgements

This work was funded by the National Research Foundation of Korea under the Basic Science Research Program (2016R1A2B4008470). Dr. S.-W. Han was financially supported by Initiative for Biological Function & Systems under the BK21 PLUS program of Korean Ministry of Education.

Keywords: ω-transaminase • chiral amines • asymmetric synthesis • enzyme assay • substrate profiling

[1] a) T. C. Nugent, *Chiral Amine Synthesis: Methods, Developments and Applications*, Wiley-VCH, Weinheim, **2010**; b) U. T. Bornscheuer, G. W. Huisman, R. J. Kazlauskas, S. Lutz, J. C. Moore, K. Robins, *Nature* **2012**, *484*, 185-194; c) M. Breuer, K. Ditrich, T. Habicher, B. Hauer, M. Kesseler, R. Sturmer, T. Zelinski, *Angew. Chem. Int. Ed.* **2004**, *43*, 788-824; d) V. Gotor-Fernández, V. Gotor, *Curr. Opin. Drug Discov. Devel.* **2009**, *12*, 784-797.

[2] T. C. Nugent, M. El-Shazly, *Adv. Synth. Catal.* **2010**, *352*, 753-819.

[3] D. Ghislieri, N. J. Turner, *Top. Catal.* **2014**, *57*, 284-300.

[4] a) L. D. Tran, O. Daugulis, *Angew. Chem. Int. Ed.* **2012**, *51*, 5188-5191; b) S. J. Zuend, M. P. Coughlin, M. P. Lalonde, E. N. Jacobsen, *Nature* **2009**, *461*, 968-970.

[5] a) M. S. Malik, E. S. Park, J. S. Shin, *Appl. Microbiol. Biotechnol.* **2012**, *94*, 1163-1171; b) R. C. Simon, N. Richter, E. Busto, W. Kroutil, *ACS Catal.* **2014**, *4*, 129-143; c) F. Guo, P. Berglund, *Green Chem.* **2017**, *19*, 333-360; d) S. A. Kelly, S. Pohle, S. Wharry, S. Mix, C. C. R. Allen, T. S. Moody, B. F. Gilmore, *Chem. Rev.* **2018**, *118*, 349-367.

[6] a) D. Koszelewski, K. Tauber, K. Faber, W. Kroutil, *Trends Biotechnol.* **2010**, *28*, 324-332; b) C. K. Savile, J. M. Janey, E. C. Mundorff, J. C. Moore, S. Tam, W. R. Jarvis, J. C. Colbeck, A. Krebber, F. J. Fleitz, J. Brands, P. N. Devine, G. W. Huisman, G. J. Hughes, *Science* **2010**, *329*,

305-309; c) M. Fuchs, J. E. Farnberger, W. Kroutil, *Eur. J. Org. Chem.* **2015**, *2015*, 6965-6982.

[7] a) S. Heintz, T. Börner, R. H. Ringborg, G. Rehn, C. Grey, M. Nordblad, U. Krühne, K. V. Gernaey, P. Adlercreutz, J. M. Woodley, *Biotechnol. Bioeng.* **2017**, *114*, 600-609; b) J. L. Galman, I. Slabu, N. J. Weise, C. Iglesias, F. Parmeggiani, R. C. Lloyd, N. J. Turner, *Green Chem.* **2017**, *19*, 361-366.

[8] a) D. F. A. R. Dourado, S. Pohle, A. T. P. Carvalho, D. S. Dheeman, J. M. Caswell, T. Skvortsov, I. Miskelly, R. T. Brown, D. J. Quinn, C. C. R. Allen, L. Kulakov, M. Huang, T. S. Moody, *ACS Catal.* **2016**, *6*, 7749-7759; b) S. W. Han, J. Kim, H. S. Cho, J. S. Shin, *ACS Catal.* **2017**, *7*, 3752-3762; c) I. V. Pavlidis, M. S. Weiß, M. Genz, P. Spurr, S. P. Hanlon, B. Wirz, H. Iding, U. T. Bornscheuer, *Nat. Chem.* **2016**, *8*, 1076-1082.

[9] a) K. S. Midelfort, R. Kumar, S. Han, M. J. Karmilowicz, K. McConnell, D. K. Gehlhaar, A. Mistry, J. S. Chang, M. Anderson, A. Villalobos, J. Minshull, S. Govindarajan, J. W. Wong, *Protein Eng. Des. Sel.* **2013**, *26*, 25-33; b) A. Nobili, F. Steffen‐Munsberg, H. Kohls, I. Trentin, C. Schulzke, M. Höhne, U. T. Bornscheuer, *ChemCatChem* **2015**, *7*, 757-760; c) S. W. Han, E. S. Park, J. Y. Dong, J. S. Shin, *Adv. Synth. Catal.* **2015**, *357*, 1732-1740; d) K. E. Cassimjee, M. S. Humble, H. Land, V. Abedi, P. Berglund, *Org. Biomol. Chem.* **2012**, *10*, 5466-5470; e) M. S. Weiß, I. V. Pavlidis, P. Spurr, S. P. Hanlon, B. Wirz, H. Iding, U. T. Bornscheuer, *ChemBioChem* **2017**, *18*, 1022-1026; f) M. S. Weiß, I. V. Pavlidis, P. Spurr, S. P. Hanlon, B. Wirz, H. Iding, U. T. Bornscheuer, *Org. Biomol. Chem.* **2016**, *14*, 10249-10254.

[10] a) S. Schätzle, M. Höhne, K. Robins, U. T. Bornscheuer, *Anal. Chem.* **2010**, *82*, 2082-2086; b) M. S. Weiß, I. V. Pavlidis, C. Vickers, M. Hohne, U. T. Bornscheuer, *Anal. Chem.* **2014**, *86*, 11847-11853; c) J. Hopwood, M. D. Truppo, N. J. Turner, R. C. Lloyd, *ChemComm* **2011**, *47*, 773-775; d) S. C. Willies, J. L. Galman, I. Slabu, N. J. Turner, *Phil. Trans. R. Soc. A* 2016, 374, 20150084.

[11] a) S. Schätzle, M. Höhne, E. Redestad, K. Robins, U. T. Bornscheuer, *Anal. Chem.* **2009**, *81*, 8244-8248; b) M. D. Truppo, J. D. Rozzell, J. C. Moore, N. J. Turner, *Org. Biomol. Chem.* **2009**, *7*, 395-398; c) M. D. Truppo, N. J. Turner, *Org. Biomol. Chem.* **2010**, *8*, 1280-1283; d) A. P. Green, N. J. Turner, E. O'Reilly, *Angew. Chem. Int. Ed.* **2014**, *53*, 10714-10717; e) D. Baud, N. Ladkau, T. S. Moody, J. M. Ward, H. C. Hailes, *ChemComm* **2015**, *51*, 17225-17228; f) A. Dunbabin, F. Subrizi, J. M. Ward, T. D. Sheppard, H. C. Hailes, *Green Chem.* **2017**, *19*, 397-404; g) T. Scheidt, H. Land, M. Anderson, Y. Chen, P. Berglund, D. Yi, W. D. Fessner, *Adv. Synth. Catal.* **2015**, *357*, 1721-1731.

[12] a) L. Leipold, D. Dobrijevic, J. W. E. Jeffries, M. Bawn, T. S. Moody, J. M. Ward, H. C. Hailes, *Green Chem.* **2019**, *21*, 75-86; b) M. Gustavsson, M. N. Muraleedharan, G. Larsson, *Appl. Environ. Microbiol.* **2014**, *80*, 2293-2298.

[13] a) F. Steffen-Munsberg, C. Vickers, A. Thontowi, S. Schätzle, T. Tumlirsch, M. S. Humble, H. Land, P. Berglund, U. T. Bornscheuer, M. Höhne, *ChemCatChem* **2013**, *5*, 150-153; b) E. S. Park, J. Y. Dong, J. S. Shin, *Appl. Microbiol. Biotechnol.* **2014**, *98*, 651-660; c) U. Kaulmann, K. Smithies, M. E. B. Smith, H. C. Hailes, J. M. Ward, *Enzyme Microb. Technol.* **2007**, *41*, 628-637; d) E.-S. Park, M. Kim, J.-S. Shin, *Appl. Microbiol. Biotechnol.* **2012**, *93*, 2425-2435; e) J. S. Shin, B. G. Kim, J *Org. Chem.* **2002**, *67*, 2848-2853.

[14] E. S. Park, J. Y. Dong, J. S. Shin, *Org. Biomol. Chem.* **2013**, *11*, 6929-6933.

[15] a) K. M. Mayer, F. H. Arnold, *J. Biomol. Screen.* **2002**, *7*, 135-140; b) C. V. Agu, S. M. Lai, V. Ujor, P. K. Biswas, A. Jones, V. Gopalan, T. C. Ezeji, *Sci. Rep.* **2018**, *8*, 3379.

[16] S. Watanabe, T. Kodaki, K. Makino, *J. Biol. Chem.* **2006**, *281*, 28876-28888.

[17] R. A. Alberty, A. Cornish-Bowden, *Trends Biochem. Sci.* **1993**, *18*, 288-291.

[18] E. S. Park, S. Park, J. S. Shin, *J. Biosci. Bioeng.* **2017**, *123*, 528-533.

[19] S. W. Han, E. S. Park, J. Y. Dong, J. S. Shin, *Adv. Synth. Catal.* **2015**, *357*, 2712-2720.

[20] A. Iwasaki, K. Matsumoto, J. Hasegawa, Y. Yasohara, *Appl. Microbiol. Biotechnol.* **2012**, *93*, 1563-1573.

[21] V. Ponti, M. U. Dianzani, K. Cheeseman, T. F. Slater, *Chem. Biol. Interact.* **1978**, *23*, 281-291.

[22] P. Christen, P. K. Mehta, *Chem. Rec.* **2001**, *1*, 436-447.

[23] R. Percudani, A. Peracchi, *BMC Bioinform.* **2009**, *10*, 273.

[24] E. S. Park, S. R. Park, S. W. Han, J. Y. Dong, J. S. Shin, *Adv. Synth. Catal.* **2014**, *356*, 212-220.

[25] a) M. D. Toney, *Arch. Biochem. Biophys.* **2014**, *544*, 119-127; b) K. Hirotsu, M. Goto, A. Okamoto, I. Miyahara, *Chem. Rec.* **2005**, *5*, 160-172.

[26] a) C. Rausch, A. Lerchner, A. Schiefner, A. Skerra, *Proteins* **2013**, *81*, 774-787; b) L. J. Guan, J. Ohtsuka, M. Okai, T. Miyakawa, T. Mase, Y. Zhi, F. Hou, N. Ito, A. Iwasaki, Y. Yasohara, M. Tanokura, *Sci. Rep.* **2015**, *5*, 10753.

[27] E. F. Oliveira, N. M. Cerqueira, P. A. Fernandes, M. J. Ramos, *J. Am. Chem. Soc.* **2011**, *133*, 15496-15505.

[28] C. K. Yeung, A. Yep, G. L. Kenyon, M. J. McLeish, *Biochim. Biophys. Acta* **2008**, *1784*, 1248-1255.

[29] E. S. Park, M. S. Malik, J. Y. Dong, J. S. Shin, *ChemCatChem* **2013**, *5*, 1734-1738.

[30] T. A. Little, *BioPharm Int.* **2015**, *28*, 48-51.

10.1002/cctc.201900399

WILEY-VCH

FULL PAPER

Naked-eye detection: Spectrophotometric and colorimetric assay of ω-transaminase activities has been developed using aldehyde dehydrogenase as a reporter, enabling rapid substrate profiling for ketones.

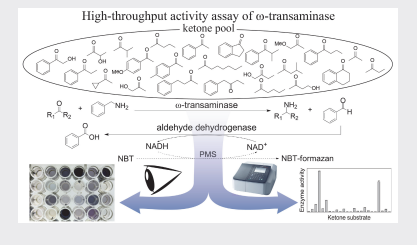

*Sang-Woo Han and Jong-Shik Shin**

Page No. – Page No.

Rapid and Quantitative Profiling of Substrate Specificity of ω-Transaminases for Ketones